Electronic Supplementary Material (ESI) for Lab on a Chip.

Electronic Supplementary Information (ESI)

ESI Figures

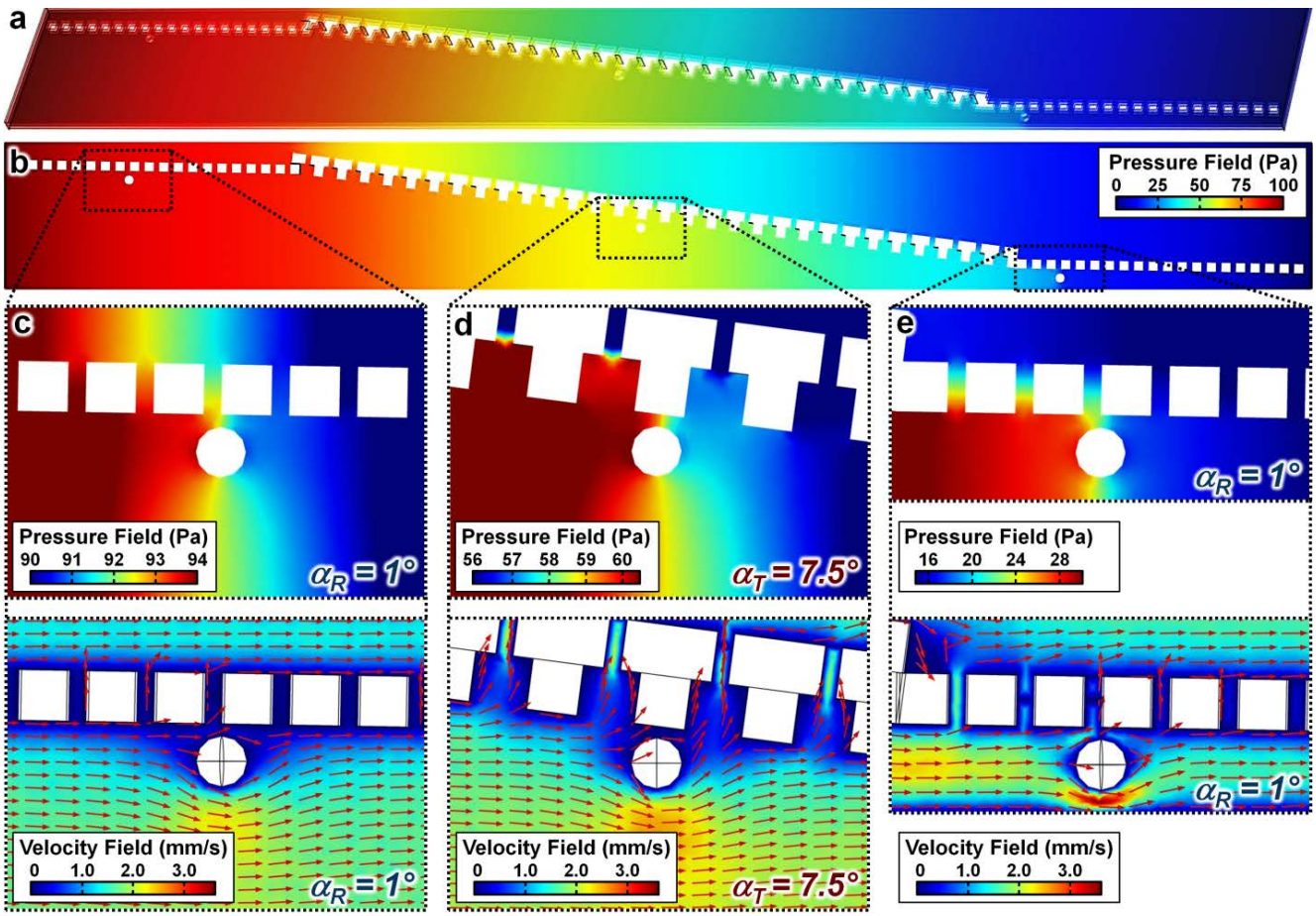

ESI Fig. 1 Three-dimensional COMSOL Multiphysics simulation results for the microfluidic "rail-trap-and-rail" system. (a) Three-dimensional pressure field view. (b) Top view at half the height of the system. (c-e) Expanded views of the pressure fields and corresponding velocity fields for microbeads located in the: (c) railing area preceding the trapping area, (d) trapping area, and (e) railing area succeeding the trapping area. The overlaid red arrows in the expanded velocity field views (c-e) mark the directions of the fluid velocity fields.

Three-dimensional fluid pressure field and velocity field simulations were performed using the commercial finite element analysis software, COMSOL Multiphysics version 4.3. Rigid spheres (15 μm in diameter) were used to model the microparticles. The three-dimensional "Incompressible Navier–Stokes" application mode for steady-state analysis was used for all simulations. The input and output pressures were set at 100 Pa and 0 Pa, respectively, while all other boundary conditions were set to have no-slip conditions. The mesh size was refined to ensure that the simulation results were independent of mesh size. The simulation included a mesh sizes of 1.2×10^5 tetrahedral elements. Water ($\rho = 10^3$ kg m^{-3}; $\eta = 10^{-3}$ Pa•s) was modelled in all of the fluidic simulations.

ESI Fig. 1 shows the changes in the flow dynamics within the microfluidic system at different points during the "rail-trap-and-rail" process. The pressure field simulation results revealed larger pressure drops across the arrayed trapping sites in the $\alpha_T = 7.5°$ trapping region compared to pressure drop across the microposts in both $\alpha_R = 1°$ railing sections (ESI Fig. 1a, b). Additionally, the expanded views in ESI Fig. 1c-e show the fluid velocity field vectors (*overlaid red arrows*) surrounding the microbeads, which were primarily in the horizontal direction for the $\alpha_R = 1°$ railing areas. This in is contrast to the $\alpha_T = 7.5°$ trapping area, which revealed a higher proportion of velocity field vectors directed into the trapping sites (ESI Fig. 1d). These simulation results suggest that the $\alpha_R = 1°$ sections would promote railing of suspended microbeads along the arrayed microposts, while the $\alpha_T = 7.5°$ section would be more likely to promote microbead arraying in the designated trapping positions.

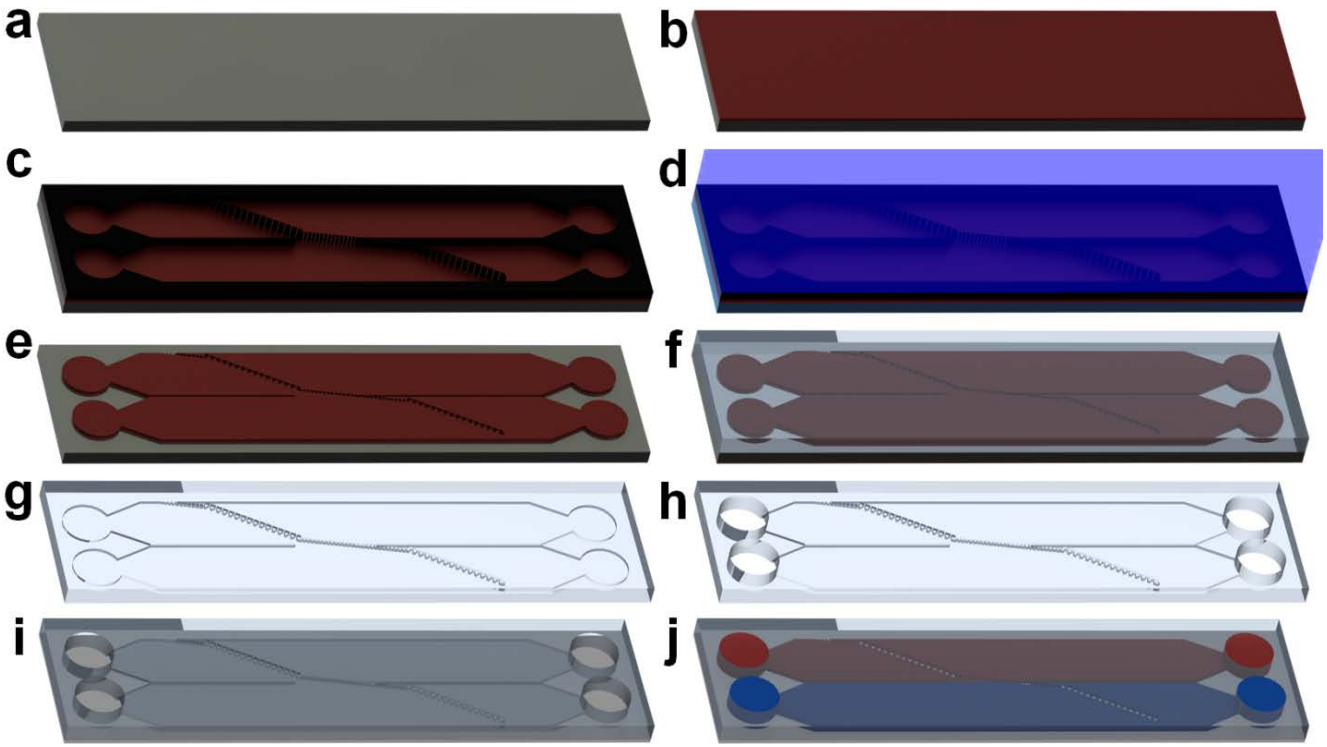

ESI Fig. 2 Conceptual illustrations of the microdevice fabrication process. (a, b) The negative photoresist, SU-8 2010 (MicroChem, Newton, MA), was spin-coated onto standard 4" Silicon wafers. (c, d) Microfeatures were defined *via* contact photolithography (Hybralign, Series 400, Optical Associates, Milpitas, CA). (e, f) Using the developed photoresist as a negative master, the device was micromolded with the silicone elastomer, poly(dimethylsiloxane) (PDMS), at a 10:1 (base : curing agent) ratio (Sylgard 184, Dow Corning, Corning, NY). (g) After curing at 55 °C for at least two hours, the PDMS was removed and individual devices were cut from the PDMS. (h) Ports for the catheter couplers (Instech Laboratories, Plymouth Meeting, PA) were punched at inlet and outlet locations. (i) The PDMS devices were cleaned and covalently bonded to Fisherbrand glass microscope slides (Fisher Scientific, Pittsburgh, PA) *via* UV ozone treatment (UVO cleaner, model 42, Jetlight Company, Irvine, CA). (j) Distinct, homogenous fluidic reagents, washes, or suspensions can be loaded in parallel.

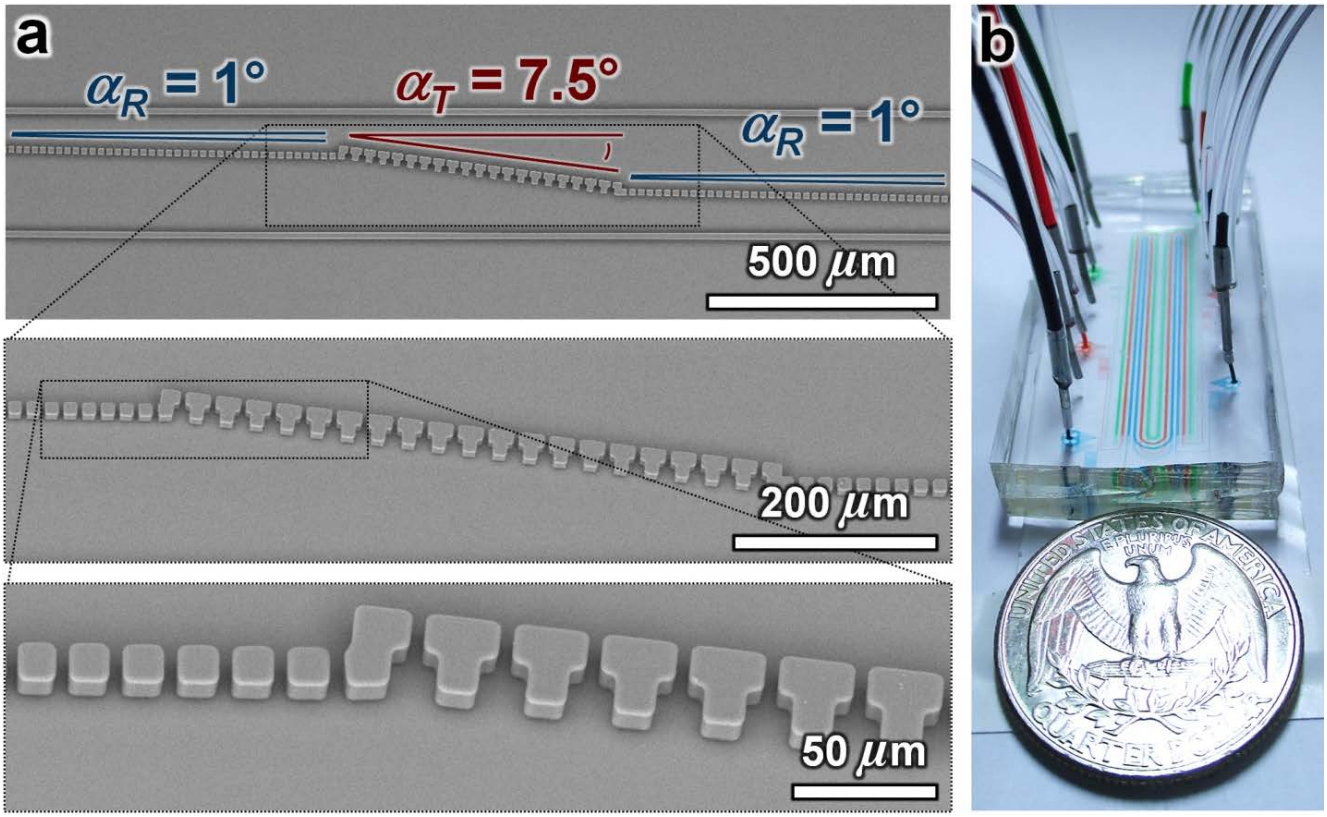

ESI Fig. 3 Microfabrication results for the microfluidic rail-trap-and-rail systems. (a) SEM micrographs. (b) Photograph of the continuous flow microfluidic reactor for detecting interferon-gamma (IFN-γ) *via* an aptamer beacon-based sandwich assay. The system is filled with coloured dye solutions and placed next to a US Quarter (approximately 24.3 mm in diameter).

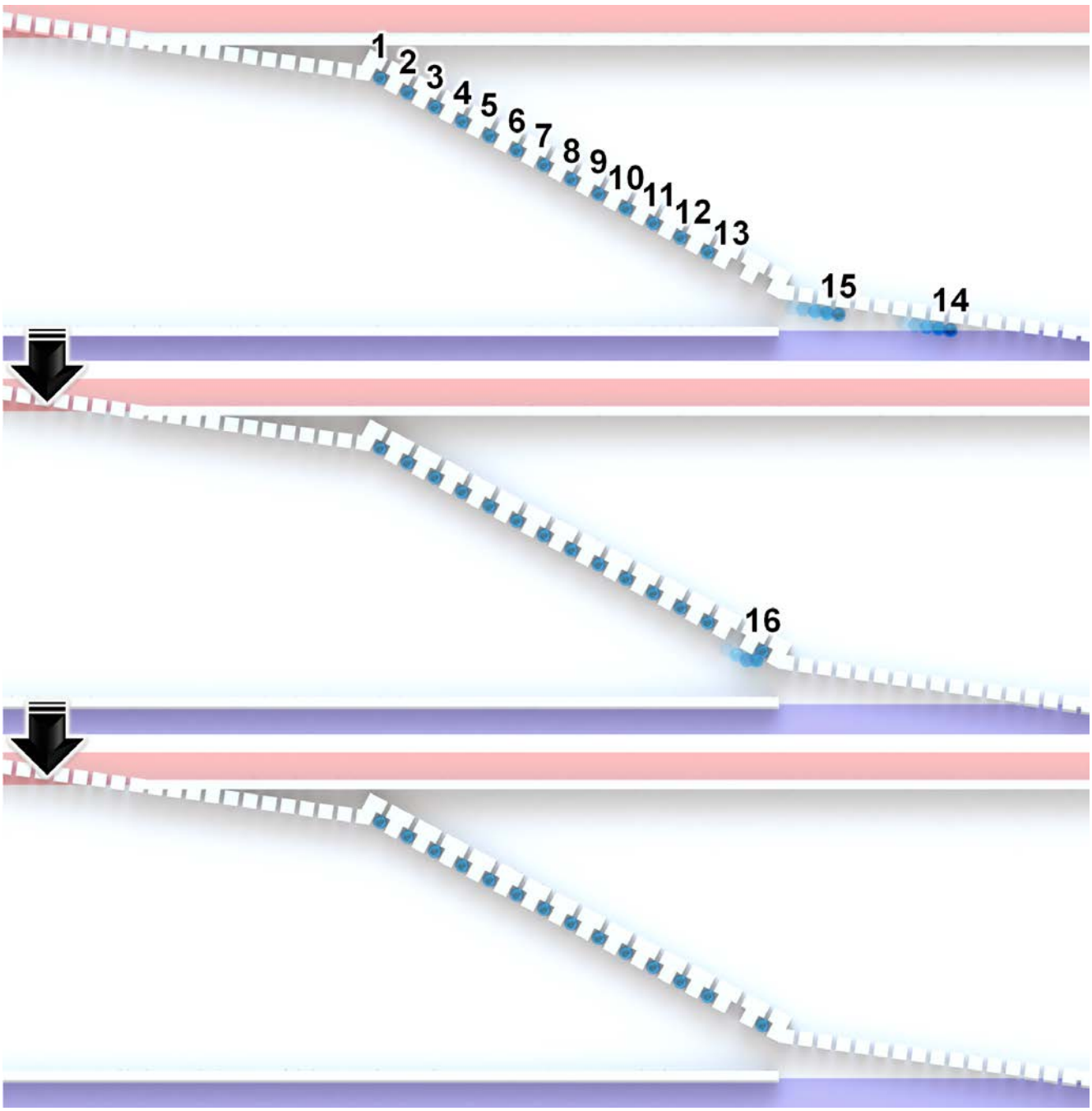

ESI Fig. 4 Conceptual examples for trapping efficiency (TE) and loading efficiency (LE) quantification. Sequential illustrations show 16 suspended microbeads being loaded into a microfluidic rail-trap-and-rail system with 15 potential trapping positions. (*Top*) Illustration showing a LE of 86.7%, corresponding to 13 of 15 loaded microbeads trapping in the 15 potential vacant trapping positions (ESI Eq. 1). (*Middle*) An additional microbead is immobilized in one of the remaining vacant trapping sites, which does not affect the LE (ESI Eq. 1). (*Bottom*) Illustration showing a TE of 93.3%, corresponding to a total of 14 microbeads immobilized in the 15 potential trapping positions following the microbead loading process (ESI Eq. 2). Microbead numbers denote the order in which each microbead was loaded into the system.

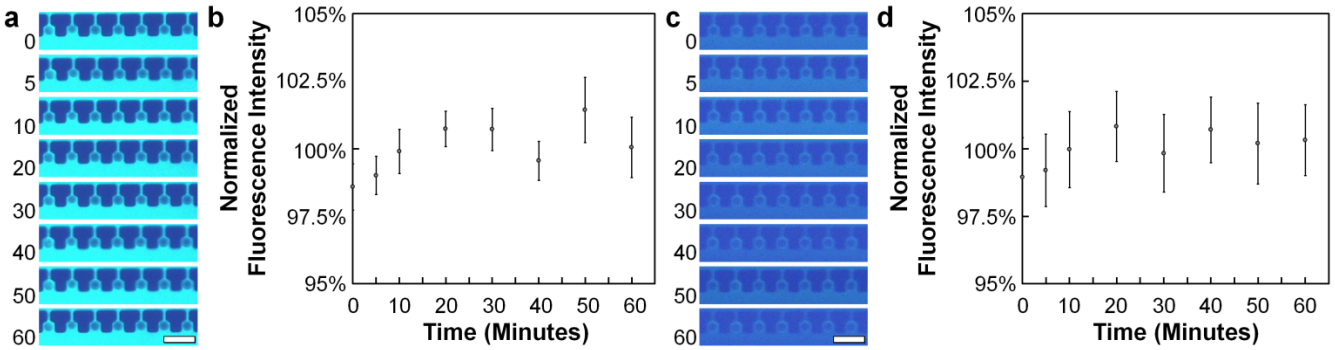

ESI Fig. 5 Experimental results for microbead-based fluorescence intensities over the course of a one hour study under continuous input flow conditions corresponding to the (a, b) "FA" and (c, d) "FA + Wash" cases. (a) Fluorescence micrographs of arrayed microbeads for the "FA" case. (b) Average normalized fluorescence intensities *versus* time for the "FA" case. (c) Fluorescence micrographs of arrayed microbeads for the "FA + Wash" case. (d) Average normalized fluorescence intensities *versus* time for the "FA + Wash" case. (a, c) Units = minutes; Scale Bars = 50 μm. (b, d) Error Bars denote s.e.m.

To investigate the potential for fluorescence signal variation associated with immobilized microbeads under continuous fluidic loading conditions, we observed and quantified the bead-based fluorescence intensities for both the "FA" and "FA + Wash" cases (ESI Fig. 5). Fluorescence micrographs corresponding to a time of 0 minutes were captured as soon as the microbead loading process was completed, which was within a time-span of approximately 5 minutes of the start of the microbead loading process. Normalized fluorescence intensities (NFIs) were calculated by normalizing the fluorescence intensities with respect to the mean of the full data set (for each independent case), which was set at 100%. Over a time-span of one hour, the continuous loading of the FA solution did not appear to affect the fluorescence signals of the immobilized microbeads, which exhibited average NFIs within ±1.5% variation (ESI Fig. 5a, b). In addition, the difference in the average NFI at the beginning and end of the one hour experiment was not statistically significant (p = 0.31) (ESI Fig. 5b). Similarly for the "FA + Wash" case, the average NFIs differed by less than ±1% over the course of the experiment (ESI Fig. 5c, d), with an indistinguishable difference in the average NFI corresponding to the beginning and end of the one hour experiment (p = 0.49) (ESI Fig. 5d).

These results suggest that the continuous fluidic loading process did not appear to instigate fluorescence signal variation for the immobilized microbeads (ESI Fig. 5), and thus, it is unlikely that the continuous flow methodology negatively impacted evaluation of the biological assay (Fig. 4). One caveat, however, is that the fluidic assay executed in this work included biological interactions with relatively strong binding affinities (*e.g.*, streptavidin-biotin interactions). As such, future works should investigate the potential for continuous flow processes to reduce assay performance *via* biomolecular dissociation. For example, as the binding affinity associated with biological interactions and/or linkers is reduced, the potential for biomolecular pairs to dissociate (*e.g.*, detachment of the FA from the microbead substrate or the Q from the FA) could increase, leading to a loss in detectable fluorescence intensities and/or undesired performance. Although such phenomena did not appear to impact the ability for the current assay to be successfully accomplished (Fig. 4), future researchers that employ continuous flow loading methodologies such as the one presented here should ensure that the potential for dissociation events are taken into consideration during assay design and use. Additionally, a number of experimental factors could be adjusted in order to improve assay performance. In this work, we introduced a platform to passively execute multi-stage fluidic reaction processes and executed a proof-of-concept demonstration using a previously presented and characterized sandwich assay;[3] however, optimization of experimental conditions (*e.g.*, to determine limits of detection for the specific assay process or increase bead-based signal intensities) was not performed. Thus, future researchers should investigate how various experimental parameters, such as environmental temperatures, mixing/incubation times, biological linker lengths, solution concentrations, and molecular beacon designs could be optimized in order to enhance the execution of bead-based multi-stage fluidic reactions for diverse chemical and biological applications.

ESI Table

ESI Table 1 Names and Sequences (5'-3' orientation) for the Aptamer Beacon Oligonucleotides (Integrated DNA Technologies, Inc., Coralville, Iowa).[3]

Name	**Sequence**
Fluorescent Aptamer (FA)	6-FAM-TGGGGTTGGTTGTGTTGGGTGTTGTGT
Quencher (Q)	ACAACCAACCCCA-BHQ-1

ESI Equations

Microbead dynamics were characterized using previously reported equations for quantifying the efficiencies associated with microbead arraying[17] and railing[16] performance. The loading efficiency (LE) was calculated as:

$$\mathrm{LE} = \frac{N_i}{N_L} \text{ for } N_L = N_T \tag{1}$$

where N_i is the number of microbeads immobilized, and N_L is the number of microbeads loaded – with the condition that the number of beads loaded (N_L) is equivalent to the number of potential trapping sites that could have been occupied (N_T).[17] For the microfluidic rail-trap-and-rail testing systems, both N_L and N_T were 20.

The trapping efficiency (TE) was calculated as:

$$\mathrm{TE} = \frac{N_a}{N_T} \tag{2}$$

where N_a is the number of microbeads successfully arrayed in the designated trapping sites, and N_T is the total number of potential trapping sites that could have been occupied. "One bead per trap" arraying refers to cases in which only one microbead is immobilized in a trapping site. "Multiple beads per trap" arraying refers to cases in which at least one microbead is immobilized in a trapping site, such as when additional beads are immobilized on top of previously arrayed microbeads.[17]

Railing Failure Rates (RFRs) associated with the microfluidic rail-trap-and-rail testing system experiments were quantified as:

$$\mathrm{RFR} = \frac{N_B}{N_G} \tag{3}$$

where N_B is the number of microbeads that ultimately immobilized in the gaps between microposts (or on top of previously immobilized microbeads), and N_G is the total number of potential gaps between microposts where the inputted microbeads could have been immobilized. Thus, an ideal microfluidic railing system would yield a *RFR* of 0%, a system in which a single microbead immobilized in every potential gap between microposts would yield a *RFR* of 100%, and a system in which microbeads consistently immobilized on top of other previously immobilized microbeads would yield a *RFR* greater than 100%.[16]

To quantify the fluorescence results, the Relative Fluorescence Intensity (RFI) for each individual microbead was calculated as:

$$\mathrm{RFI}_i = \frac{x_i - \bar{x}_Q}{\bar{x}_{FA} - \bar{x}_Q} \tag{4}$$

where x_i is the fluorescent intensity of a single microbead, $\bar{x}_Q$ is the mean fluorescent intensity of the microbeads corresponding to the Q solution for the corresponding experiment, and $\bar{x}_{FA}$ is the mean fluorescence intensity of the microbeads corresponding to the FA solution for the corresponding experiment. The calculation of RFI values normalized the fluorescence results such that the mean RFI for the FA case was set at 100%, while the mean RFI for the Q case was set at 0%. The *p* values corresponding to differences in RFI were calculated *via* unpaired *Student's t tests* because the fluorescence results associated with each reaction stage were not assumed to be distinct. Differences with *p* values that were less than 0.05 were considered statistically significant.

ESI Movie Captions

ESI Movie 1 Video of microbeads (15 μm in diameter) in the continuous flow bead-based microfluidic reactor for detecting interferon-gamma (IFN-γ) *via* an aptamer beacon-based sandwich assay: (*i*) railing from the microbead suspension into the fluorescent aptamer (FA) solution, (*ii*) arraying in the designated trapping sites in the FA solution, (*iii*) railing from the FA solution to the wash solution, (*iv*) arraying in the designated trapping sites in the wash solution, (*v*) railing from the wash solution to the quencher (Q) solution, (*vi*) arraying in the designated trapping sites in the Q solution, (*vii*) railing from the Q solution to the wash solution, (*viii*) arraying in the designated trapping sites in the wash solution, (*ix*) railing from the wash solution to the IFN-γ solution, (*x*) arraying in the designated trapping sites in the IFN-γ solution. α_R = 1°; α_T = 7.5°.

ESI Movie 2 Video of microbead dynamics in a microfluidic "rail-trap-and-rail" testing system with α_R = 1° and α_T = 5°.

ESI Movie 3 Video of microbead dynamics in a microfluidic "rail-trap-and-rail" testing system with α_R = 1° and α_T = 10°.